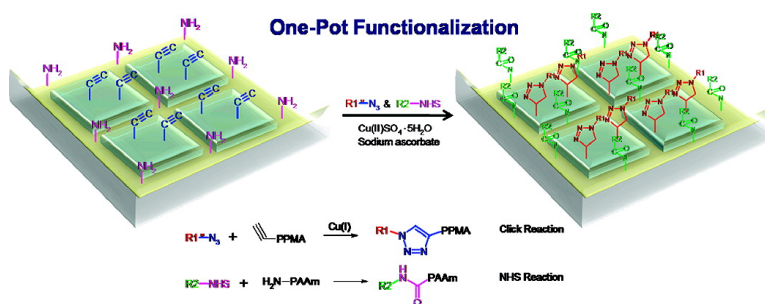


## Patterning Nanodomains with Orthogonal Functionalities: Solventless Synthesis of Self-Sorting Surfaces

Sung Gap Im, Ki Wan Bong, Byeong-Su Kim, Salmaan H. Baxamusa,  
 Paula T. Hammond, Patrick S. Doyle, and Karen K. Gleason

*J. Am. Chem. Soc.*, **2008**, 130 (44), 14424-14425 • DOI: 10.1021/ja806030z • Publication Date (Web): 08 October 2008

Downloaded from <http://pubs.acs.org> on February 8, 2009



### More About This Article

Additional resources and features associated with this article are available within the HTML version:

- Supporting Information
- Access to high resolution figures
- Links to articles and content related to this article
- Copyright permission to reproduce figures and/or text from this article

[View the Full Text HTML](#)

## Patterning Nanodomains with Orthogonal Functionalities: Solventless Synthesis of Self-Sorting Surfaces

Sung Gap Im, Ki Wan Bong, Byeong-Su Kim, Salmaan H. Baxamusa, Paula T. Hammond, Patrick S. Doyle, and Karen K. Gleason\*

Department of Chemical Engineering and Institute for Soldiers Nanotechnology, Massachusetts Institute of Technology, Cambridge, Massachusetts 02139

Received August 8, 2008; E-mail: kkg@mit.edu

Designed bioactive patterned functional surfaces can offer advantageous properties such as controlled adsorption and site-specific affinity.<sup>1,2</sup> In particular, area-selective functionalization of multiple components onto a predesigned surface<sup>2–6</sup> is highly desirable. Such a system can be utilized to detect and identify more than one analyte in biosensor applications, which enables fabrication of more effective biodevices.<sup>3</sup> Moreover, the multifunctional surface can be used as a template to monitor the interaction among the adsorbed components from a complex mixture, such as an extracellular environment. To achieve this goal, a highly efficient, orthogonal functionalization scheme with high fidelity is desirable.

Although various multicomponent patterning strategies are well-established for semiconductor industries, the direct application of these schemes for bioactive platforms is still challenging because many biological components such as proteins and nucleic acids are susceptible to degradation during patterning.<sup>7</sup> For example, conventional photolithography (PL) utilizes harsh organic solvents and UV irradiation that can potentially lead to the destruction of bioactivity.<sup>3,7</sup> Soft lithography techniques often result in the dehydration of biofunctionalities during the inking of stamps.<sup>6</sup> For these reasons, patterned surfaces had been primarily functionalized only with one component on a selected area.<sup>8,9</sup> To achieve bioactive multifunctional surfaces, J. Katz et al. synthesized a new photosensitive terpolymer that can be processed under mild biocompatible conditions;<sup>3</sup> however, the process involves a complicated synthesis. J. M. Slocik et al. used shadow mask patterning and plasma enhanced chemical vapor deposition (PECVD) for patterning of multiple components, but the resolution does not reach the nanometer scale domain and the use of thiol agents limits the type of substrates that can be used.<sup>5</sup> For nanometer scale multifunctional surfaces, a solventless patterning process that can be performed under mild conditions using commercial reactants is highly desirable.

In this report, we propose a facile solventless method for synthesizing nanopatterned multifunctional surfaces. One nanodomain contains an acetylene group which can be functionalized via click chemistry. The other nanodomain contains surface amine groups which can be functionalized by carbodiimide chemistry with *N*-hydroxysuccinimide (NHS).<sup>4,8</sup> Both the click reaction and amine functionalization (NHS reaction, afterward) are well-understood and have attractive characteristics such as high selectivity, high yield, fast reaction in aqueous phase at room temperature, and biocompatibility.<sup>4,8</sup> Moreover, the click and NHS reactions are highly orthogonal to each other so that nonspecific immobilization can be minimized.<sup>4</sup> With these functionalities, we demonstrated the covalent functionalization of two independent components in a one-pot, self-sorted area-selective process, performed in an aqueous solution at room temperature, having conditions which are biocompatible. Considering the versatility and generality of the thin

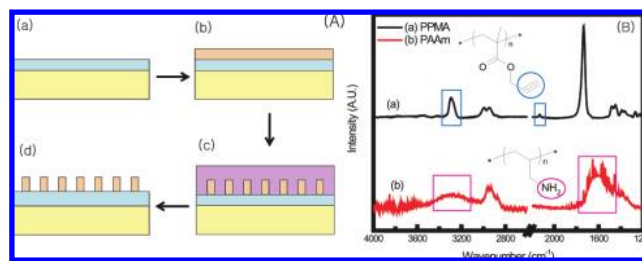


**Figure 1.** (A) Schematic procedure of nanopattern fabrication: (a) PECVD of PAAm; (b) iCVD of PPMA; (c) apply CFL mold to induce capillary rise; (d) remove CFL mold to complete the nanopattern. (B) FTIR spectra of (a) iCVD PPMA and (b) PECVD PAAm.

film deposition methods used here, we believe this platform can be easily extended to various biodevice applications.

In Figure 1A, capillary force lithography (CFL)<sup>10</sup> nanopatterns the upper layer of a bilayer structure, exposing regions of the bottom material, thus creating a dual functional surface. Cross-linking allows the bottom layer to remain immobile during the CFL step. Vapor deposition allows the insoluble bottom layer to be directly synthesized. For the top layer, the use of solventless vapor deposition is also critical, as solvents used in conventional solution processing have the potential to dissolve the underlying layer of a multilayer.<sup>11</sup> Additionally, residual solvent can lead to a biocompatibility issues.<sup>12</sup> In contrast to conventional photolithography, CFL does not require resists, developers, solvents, or chemically destructive irradiation that can deactivate the reactive functional groups.<sup>10</sup> Moreover, since the patterning process of CFL utilizes solely thermal movement of polymer film regardless of the chemical properties of polymer films, we believe this procedure can be applicable to many different sets of functional polymer films.

To create a bilayer with amine and acetylenic functional groups, first a 100 nm thick poly(allylamine) (PAAm) film using PECVD to achieve cross-linking was synthesized. Next, a 50 nm thick noncross-linked poly(propargyl methacrylate) (PPMA) film was synthesized via initiated chemical vapor deposition (iCVD). Conveniently, the monomers required for both layers are commercially available.

The Fourier Transform Infrared (FTIR) spectrum (Figure 1B) clearly shows the N–H stretching peak ( $\sim 3200\text{ cm}^{-1}$ ) and the N–C stretching peak ( $\sim 1650\text{ cm}^{-1}$ ), demonstrating retention of the amine functionality in the PECVD PAAm layer.<sup>13</sup> Similarly, the characteristic peaks of the acetylene group (C–H stretch peak at  $\sim 3300\text{ cm}^{-1}$  and C≡C stretch peak at  $\sim 2100\text{ cm}^{-1}$ )<sup>13</sup> were clearly observed in the FTIR spectrum of iCVD PPMA. The PECVD film was insoluble in common solvents for PAAm including water, methanol, and acetone, suggesting the presence of cross-linking commonly found in plasma deposited materials.<sup>14</sup>

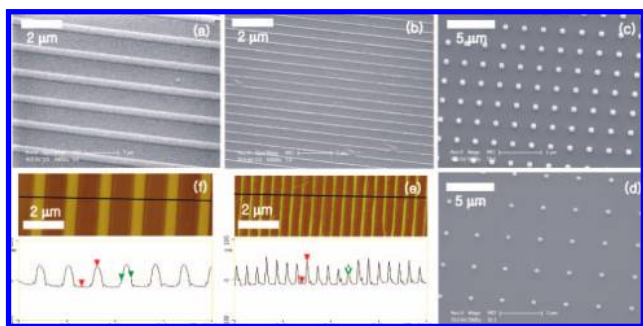


**Figure 2.** Scanning electron microscope (SEM) and atomic force microscopy (AFM) images of nanopatterned platform of iCVD PPMA on PECVD PAAm background film via CFL: SEM images of (a) 500 nm and (b) 110 nm stripe pattern; (c) 800 nm and (d) 500 nm dot patterns. AFM images of (e) 110 nm and (f) 500 nm line pattern. AFM image clearly demonstrates the pattern fidelity and exposure of PAAm of the structure.

The iCVD PPMA films were soluble in acetone and dimethylformamide (DMF), suggesting limited or no cross-linking resulted from this less energetic vapor deposition method.<sup>14</sup>

For the CFL,<sup>10</sup> a poly(dimethylsiloxane) (PDMS) or a poly(urethaneacrylate) (PUA) mold<sup>15</sup> was placed on the PPMA/PAAm/Si substrate and a pressure of  $\sim 0.1$  bar was applied to selectively induce the capillary rise of the PPMA layer. In general, a polymer film starts to deform when the temperature is raised beyond its  $T_g$ . The PECVD PAAm film showed no detectable deformation when heated up to 110 °C. Considering that the reported glass transition temperature ( $T_g$ ) of standard PAAm is  $-6$  °C,<sup>16</sup> the above results confirm that the PECVD PAAm film is highly cross-linked. On the other hand, a distinctive deformation was observed when the PPMA film was heated above 60 °C. After 30 min of pressing the CFL mold at the optimal temperature of 105 °C, well-resolved patterns were obtained over a 2 mm  $\times$  3 mm area (Figure 2). The minimum feature size obtained was 110 nm. Highly anisotropic patterns were produced with high fidelity to the mold. Line-and-space patterns, dot arrays, and complex patterns were also obtained.

The orthogonal amine and acetylene functionalities on the surface enable the self-sorting of the two fluorescent dyes onto the nanopatterned domains during a one-pot functionalization step. For the click functionalization, the red dye, tetramethylrhodamine-5-carbonyl azide (azido-rhodamine afterward,  $\lambda_{\text{abs}} = 545$  nm,  $\lambda_{\text{em}} = 578$  nm) in the presence of a Cu(I) cation catalyst forms a triazole covalent linkage to the acetylene group of the PPMA patterned domain.<sup>8</sup> For the NHS functionalization, the green dye, 5-(and 6-)carboxyfluorescein, succinimidyl ester (NHS-fluorescein afterward,  $\lambda_{\text{abs}} = 491$  nm,  $\lambda_{\text{em}} = 518$  nm) forms a covalent peptide bond with the amine group in PAAm areas. The one-pot functionalization step from a mixture of the two dyes was performed in aqueous solution at room temperature for 20 h. A small amount of DMSO was added in the solution to improve the limited solubility of azido-rhodamine in the water (v/v ratio of water to DMSO was 9:1). The functionalized nanopattern was thoroughly rinsed with water and nitrogen-dried.

The selective self-sorted pattern of fluorescent dyes was clearly observed by fluorescence microscopy (Figure 3). During the one-pot functionalization, both surface groups recognized their conjugate functionalities in the dye and thus the surface was selectively tagged by the dye according to the predesigned pattern. The overlapped

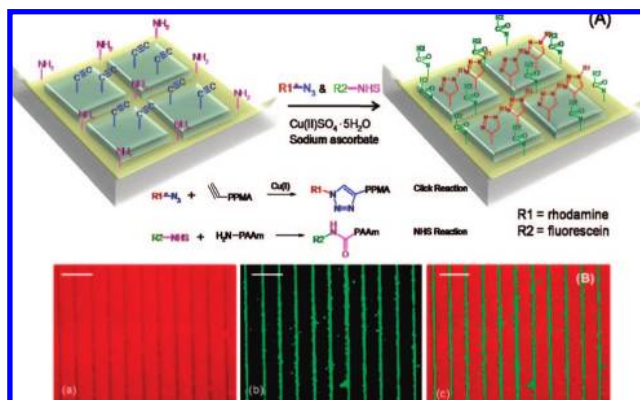


**Figure 3.** (A) Schematic procedure of one-pot functionalization. (B) Fluorescence microscope image of (a) click functionalized red dye excited at 545 nm, (b) NHS functionalized green dye excited at 491 nm, and (c) overlapped image of (a) and (b). Each scale bars represents 30  $\mu\text{m}$ .

fluorescent image clearly demonstrates that the top PPMA was completely dewetted from the bottom PAAm surface during the CFL.

In summary, we have demonstrated a dual functional nanopatterned platform with a minimum feature size of 110 nm. The fabrication process utilized sequential solventless CVD processes and was patterned by a CFL process. By applying one-pot, biocompatible functionalization, the conjugate fluorescent dyes were assembled onto the pattern in a self-sorted fashion. Considering the ease of fabrication and the versatility and orthogonality of the utilized functional groups, we believe this platform can be a powerful tool for biodevice applications in high throughput, multicomponent systems.

**Acknowledgment.** This research was supported by the U.S. Army through the Institute for Soldier Nanotechnologies, under Contract DAAD-19-02-D-0002 with the U.S. Army Research Office.

**Supporting Information Available:** Detailed experimental procedures. This material is available free of charge via the Internet at <http://pubs.acs.org>.

## References

- (1) Nie, Z.; Kumacheva, E. *Nat. Mater.* **2008**, *7*, 277.
- (2) Xu, H.; Hong, R.; Lu, T. X.; Uzun, O.; Rotello, V. M. *J. Am. Chem. Soc.* **2006**, *128*, 3162.
- (3) Katz, J. S.; Doh, J.; Irvine, D. J. *Langmuir* **2006**, *22*, 353.
- (4) Malkoch, M.; Thibault, R. J.; Drockenmuller, E.; Messerschmidt, M.; Voit, B.; Russell, T. P.; Hawker, C. J. *J. Am. Chem. Soc.* **2005**, *127*, 14942.
- (5) Slocik, J. M.; Beckel, E. R.; Jiang, H.; Enlow, J. O.; Zabinski, J. S.; Bunning, T. J.; Naik, R. R. *Adv. Mater.* **2006**, *18*, 2095.
- (6) Zhou, F.; Zheng, Z. J.; Yu, B.; Liu, W. M.; Huck, W. T. S. *J. Am. Chem. Soc.* **2006**, *128*, 16253.
- (7) Sorribas, H.; Padeste, C.; Tiefenauer, L. *Biomaterials* **2002**, *23*, 893.
- (8) Lutz, J. F. *Angew. Chem., Int. Ed.* **2007**, *46*, 1018.
- (9) Suh, K. Y.; Langer, R.; Lahann, J. *Adv. Mater.* **2004**, *16*, 1401.
- (10) Suh, K. Y.; Lee, H. H. *Adv. Funct. Mater.* **2002**, *12*, 405.
- (11) Chan, K.; Gleason, K. K. *J. Electrochem. Soc.* **2006**, *153*, C223.
- (12) O'Shaughnessy, W. S.; Murthy, S. K.; Edell, D. J.; Gleason, K. K. *Biomacromolecules* **2007**, *8*, 2564.
- (13) Lin-Vien, D. *The Handbook of Infrared and Raman Characteristic Frequencies of Organic Molecules*; Academic Press: Boston, 1991.
- (14) Tenhaeff, W. E.; Gleason, K. K. *Adv. Funct. Mater.* **2008**, *18*, 979.
- (15) Kim, Y. S.; Baek, S. J.; Hammond, P. T. *Adv. Mater.* **2004**, *16*, 581.
- (16) Stone, F. W.; Stratta, J. J. *Encyclopedia of Polymer Science and Technology*; Union Carbide Corp.: 2002; Vol. 6.

JA80630Z